



Comparison of measurement and prediction for acoustical treatments designed with Transfer Matrix Models

Rinaldi Petrolli¹, Artur Zorzo¹, Peter D'Antonio^{1,2}

¹ REDI Acoustics, LLC, USA

rinaldi.petrolli@rediacoustics.com, artur.zorzo@rediacoustics.com, peter.dantonio@rediacoustics.com

² RPG Acoustic Systems, LLC, USA

dr.peter.dantonio@gmail.com, pdantonio@rpgacoustic.com

Abstract

As part of the Non-cuboid Iterative Room Optimizer program development, in addition to optimizing the room's geometry to obtain a flat modal response, a module adding low-frequency absorption was added to further improve the response. A variety of pressure and velocity absorbers of different designs were investigated. This paper compares impedance tube measurements and predictions, using the Transfer Matrix Models. Additional prediction models for modeling different face plates and resistive cavity absorption are also examined. Examples using a 16 cm² tube with a response between 63 Hz and 4000 Hz and a 60 cm² tube, with a response between 20 Hz and 200 Hz, will be discussed. Both porous absorbers and pressure absorbers are evaluated.

Keywords: transfer matrix model, acoustic treatments, surface impedance.

1 Introduction

Controlling low-frequency room modes is a critical step in a proper design of a studio or listening room. Even though the theory regarding low-frequency absorbers like membranes and different types of Helmholtz resonators is well established, obtaining reliable measurements to verify the analytical models and the construction aspects, especially in frequencies below 100 Hz, has been an issue to acousticians and acoustic equipment manufacturers.

One of the main problems is that several simplifications are made in the analytical modeling approaches and many construction details and techniques are not considered in the design equations. Another issue is to find a suitable measurement method, which can become difficult when there is a need for precision at low-frequencies. For impedance tubes, the area and length of the tube have to be quite big to provide reliable results at lower frequencies.

In an effort to confirm the validity of the low-frequency absorbers design methods on the Non-cuboid Iterative Room Optimizer (NIRO) software [7], several absorbers were built and measured, using two different

impedance tubes. The software uses the Transfer Matrix Model to design and predict the complex surface impedance of different resonators. An open-source python toolbox for designing and predicting several types of acoustic absorbers was created as part of the software and can be found in [6]. The method will be described in detail in the next section.

2 Transfer Matrix Model

The Transfer Matrix Model (TMM) representation, also known as four-pole parameter representation or transmission matrix, enables the calculation of the surface impedance of single and multiple layered treatments by considering the continuity of pressure and velocity from one layer to the next, thus enabling the use of surface impedance of one layer as the backing surface of the next. The method works by representing the acoustical properties of the device through its four-pole parameters, which relate pressure and particle velocity on each side of each layer of the device. Consider the acoustic device shown in Figure 1a, the transfer matrix of the single layer e_1 can be defined as

$$\begin{bmatrix} p_{in} \\ u_{in} \end{bmatrix} = \begin{bmatrix} A_1 & B_1 \\ C_1 & D_1 \end{bmatrix} \begin{bmatrix} p_{out} \\ u_{out} \end{bmatrix}, \quad (1)$$

where p_{in} , p_{out} and u_{in} , u_{out} are pressure and particle velocity on each side of the layer and A_1 , B_1 , C_1 and D_1 are the four-pole parameters.

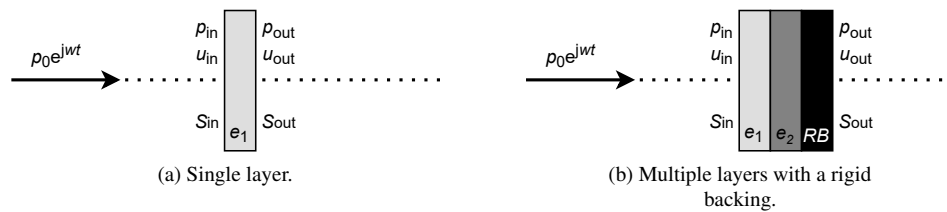


Figure 1 – Composition of single and multi-layered acoustical treatments.

A multilayered system can be represented by adding the four-pole parameters of the other layers, which for a double layer device results in the following matrix:

$$T_G = \begin{bmatrix} A_1 & B_1 \\ C_1 & D_1 \end{bmatrix} \begin{bmatrix} A_2 & B_2 \\ C_2 & D_2 \end{bmatrix} = \begin{bmatrix} A_G & B_G \\ C_G & D_G \end{bmatrix}, \quad (2)$$

in which A_2 , B_2 , C_2 and D_2 are the four-pole parameters of the second layer. The multiplication of these matrices can be defined as the global transfer matrix T_G with A_G , B_G , C_G and D_G as the global four-pole

parameters. With the global transfer matrix, the surface impedance at the top layer can be calculated as [8]:

$$Z_{in} = S_{in} \frac{B_G + A_G \widetilde{Z}_{out} / S_{out}}{D_G + C_G \widetilde{Z}_{out} / S_{out}}, \quad (3)$$

where S_{in} and S_{out} are the surface areas of the first and last layers and \widetilde{Z}_{out} is the radiation impedance at the last layer. If the last layer has a rigid backing ($u_{out} = 0$ and $\widetilde{Z}_{out} \rightarrow \infty$), as shown in Figure 1b, the surface impedance can be defined as $Z_{in} = S_{in} \frac{A_G}{C_G}$.

The treatment samples that will be analyzed in this work will require only two different type of four-pole parameters matrices: one for equivalent fluid elements and one for barrier type elements. The first is used to describe both air and porous material layers and the latter is used to represent thin plates, such as perforated/slotted plates and membranes. The four-pole parameters for equivalent fluids and plate type elements provided by the literature[1, 4] are, respectively:

$$T_{EF} = \begin{bmatrix} \cos(kt) & j\rho c \sin(kt) \\ j \frac{\sin(kt)}{\rho c} & \cos(kt) \end{bmatrix}, \quad (4) \quad T_B = \begin{bmatrix} 1 & Z_s \\ 0 & 1 \end{bmatrix}, \quad (5)$$

where in Eq. 4 t is the layer thickness, k is the wavenumber, ρ is the density of the media, c is the speed of sound and in Eq. 5 Z_s is the complex characteristic impedance. Once the impedance is obtained, the sound absorption coefficient α can be calculated by $\alpha = 1 - |(Z - \rho_0 c) / (Z + \rho_0 c)|$, where ρ_0 is the characteristic impedance of air.

2.1 Equivalent fluid models

Several models for the prediction of the normal incidence surface impedance of porous materials, both empirical and theoretical, have been developed and published since the 1970s. While the empirical methods rely on regression models applied to many experimental measurements of different materials, the theoretical models are based on the physical considerations of the sound propagation inside the material. The use of these two types of models can be divided into three main aspects: the input parameters, the type of material they are applicable to and the frequency range in which they are valid.

While the theoretical models might be more precise due to their increased level of complexity, some required parameters, like tortuosity and porosity, are not published by manufacturers and very complicated to measure. Nevertheless, using an empirical model due to its input simplicity, *i.e.* only using the flow resistivity and material thickness as input parameters, might not yield accurate results depending on the limitations of the model. To address that, we are going to consider the findings in [5], which developed a single parameter model by formulating the theoretical model of Allard and Champoux in the same manner as other empirical methods. Their model was measured for a wool sample from 45 to 11,000 Hz. The complex characteristic impedance Z_c

and the wavenumber k_c of the model proposed in [5] are defined by:

$$Z_c = Z_0(1 + 0.0729 X^{-0.66228} - j 0.18700 X^{-0.53790}), \quad (6)$$

$$k_c = \frac{\omega}{c}(1 + 0.09820 X^{-0.68500} - j 0.28800 X^{-0.52600}), \quad (7)$$

where Z_0 is the characteristic impedance of air, ω is the angular frequency and $X = \rho_0 f / \sigma$ with f being frequency in Hz and σ the flow resistivity of the material. Z_c and k_c are used in Eq. 4 along with the thickness t to represent a layer of porous material in the transfer matrix structure. Instead, if Z_0 and k_0 are used, with $k_0 = \omega / c_0$, Eq. 4 can also represent an air layer given its thickness t .

2.2 Perforated plates

The complex characteristic impedance of a perforated plate is given by $Z_{pp} = r_{pp} + j\omega m_{pp}$ [2], in which

$$r_{pp} = \frac{\rho_0}{\epsilon_{pp}} \left[t_{corr} + \sqrt{\frac{8\eta}{\omega} \left(1 + \frac{t}{d}\right)} \right], \quad (8) \quad m_{pp} = \frac{\rho_0 t_{corr}}{\epsilon_{pp}}, \quad (9)$$

$$t_{corr} = t + \delta \frac{d}{2}, \quad (10) \quad \delta = 0.85 \left(1 - 1.13\epsilon_{pp}^{1/2} - 0.09\epsilon_{pp} + 0.27\epsilon_{pp}^{3/2}\right). \quad (11)$$

Here, t_{corr} is the end correction and δ is Jaouen and Bécot's formulation for circular holes in a square pattern. In addition, d is the hole diameter, t is the panel thickness, η is the air viscosity coefficient and ϵ_{pp} represents the ratio of the perforated hole area to the panel area. Z_{pp} is used in Eq. 5 to represent a perforated plate in the transfer matrix structure.

3 Methodology

This section will describe the measurement techniques and the test samples that are analyzed.

3.1 Impedance Tubes

The measurements conducted in this study were made with 2 different impedance tubes. This measurement method is based on a tube connected to a loudspeaker on one end and a test sample mounted on the other end. Plane waves are generated inside the tube by the loudspeaker and the complex surface impedance of the test sample can be derived by measuring the acoustic pressure in two or more different locations of the tube, with surface microphones, or with the microphones inside the tube, if they are small compared to the area of the tube. A diagram of the three microphone test method can be seen in Figure 2.

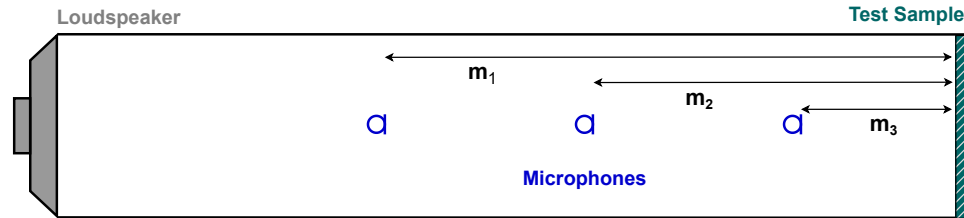


Figure 2 – Impedance tube diagram.

With m_1 , m_2 and m_3 as the positions of the microphones and k the wave number, the transfer function between the two microphones (H_{ab}) with ab being the three microphone combinations (m_1m_2 , m_2m_3 and m_1m_3), the reflection coefficient (R), the complex surface impedance (Z_1) and the absorption coefficient (α) can be easily obtained with:

$$R = \frac{H_{ab}e^{jkm_1} - e^{jkm_2}}{e^{-jkm_2} - H_{ab}e^{-jkm_1}}, \quad (12) \quad \frac{Z_1}{\rho_0 c} = \frac{1+R}{1-R}, \quad (13) \quad \alpha = 1 - |R|^2. \quad (14)$$

The measurements with the 60 cm² impedance tube were conducted in RPG's Acoustic Research Center (ARC). To obtain reliable absorption measurements down to 20 Hz, a 0.6 x 0.6 x 5.6 meter impedance tube was built in accordance with the ISO 10534-2 [3]. The apparatus is equipped with a movable microphone that can measure the pressure in three distinct positions in front of the test sample (Figure 3). The reflection factor and normal absorption coefficients are then obtained, using the transfer function between three measurement positions.

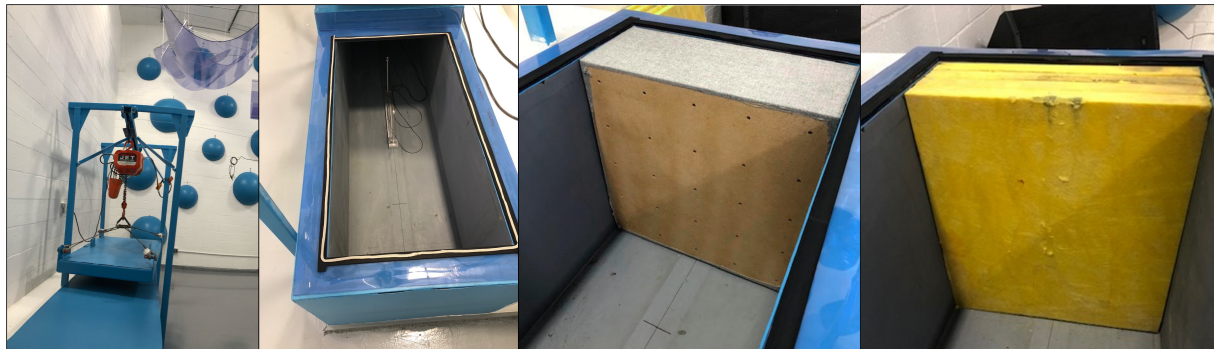


Figure 3 – ARC's impedance tube (left and middle-left). Test sample S1 (middle-right). Test sample S2 (right).

The 16 cm² impedance tube used for the experiments and a measured sample of perforated plate resonator and porous material can be seen in Figure 4. The speaker to sample distance is 1.6 m, with an adjustable rigid termination for any desired cavity depth. The frequency bandwidth is 63 Hz to 4000 Hz.



Figure 4 – 16 cm² impedance tube (top). Four-microphone measurement system (bottom-left). Test sample S5 (bottom-middle). Test sample S7 (bottom-right).

3.1.1 Frequency limitations of the impedance tube transfer-function method

According to the standard, the lower frequency limit or the working frequency range of the method depends on the spacing between the measurement microphones and the accuracy of the analysis system. As a general guide, the spacing should be defined by the following relation:

$$f_l > \frac{0.05c}{s}, \quad (15)$$

where s is the distance between the two measurement microphones and f_l is the lower frequency of interest. This means that to accurately measure absorption down to 20 Hz the microphones should be spaced at least 0.68 m from each other. It is important to note that a higher spacing will lead to more accurate measurements, hence the interest in an impedance tube with large dimensions. The maximum distance used in the ARC's impedance tube is 1.98 m, which translates to a theoretical lower frequency limit of 8.6 Hz, if the limitations of the measurement microphone are not considered. The 16 cm² impedance tube used in this study, due to its smaller size, has a low-frequency limit of 63 Hz.

The highest frequency that can be measured is defined by Equation 16. Here, d is the diameter of the tube and c is the speed of sound. This is a statement that there should not be any cross modes in the tube.

$$f_u < \frac{c}{2d}. \quad (16)$$

In order to increase the maximum measurement frequency, four microphones can be placed as shown in Figure 5. According to [2], the microphones are positioned at the null of the second order cross mode and, by

summing the microphone's signals, the first and third order cross modes in each direction are canceled. Thus, the maximum frequency is increased by a factor of four. This technique was used on the small impedance tube measurements, increasing the maximum measurable frequency up to 4000 Hz.

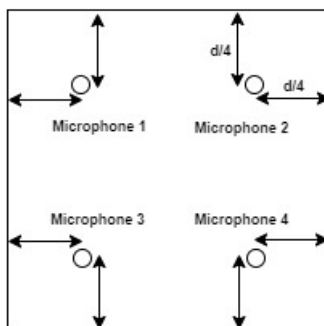


Figure 5 – Multi-mic impedance tube set-up used in the 16 cm² tube.

3.2 Measured samples

A total of 8 samples with different materials and properties were tested. A detail description of each sample, divided by layers can be seen in Table 1, in which the frequency range column is defined by the impedance tube used to measure the sample.

Table 1 – Test samples specifications - t is thickness, d is hole diameter, s is hole spacing and σ is flow resistivity. The units of t , d and s are millimeters and σ is kPa s/m².

Sample	Type	Freq. Range	Layer 1	Layer 2	Layer 3
S1	Resonator	20 - 200 Hz	Perforated Plate $t : 19.0 \mid d : 9.0 \mid s : 134.6$	R19 Fiberglass $t : 158.0 \mid \sigma : 4.0$	Air Gap $t : 50.0$
S2	Porous	20 - 200 Hz	703 Fiberglass $t : 200.0 \mid \sigma : 27.0$	-	-
S3	Porous	63 - 4000 Hz	703 Fiberglass $t : 200.0 \mid \sigma : 27.0$	-	-
S4	Resonator	63 - 4000 Hz	Perforated Plate $t : 19.0 \mid d : 6.35 \mid s : 31.7$	703 Fiberglass $t : 50.8 \mid \sigma : 27.0$	-
S5	Resonator	63 - 4000 Hz	Perforated Plate $t : 19.0 \mid d : 6.35 \mid s : 31.7$	R19 Fiberglass $t : 50.8 \mid \sigma : 4.0$	-
S6	Resonator	63 - 4000 Hz	703 Fiberglass $t : 50.8 \mid \sigma : 27.0$	Perforated Plate $t : 19.0 \mid d : 6.35 \mid s : 31.7$	R19 Fiberglass $t : 50.8 \mid \sigma : 4.0$
S7	Porous	63 - 4000 Hz	703 Fiberglass $t : 50.8 \mid \sigma : 27.0$	-	-
S8	Porous	63 - 4000 Hz	Melamine Foam $t : 100.0 \mid \sigma : 9.6$	-	-

Both fiberglass materials used in this research, R19 and 703, are commercial products produced by Owens Corning and the melamine foam is Basotect by BASF. The flow resistivity values shown here were measured by the authors.

4 Results

The measured absorption coefficients obtained for each sample were compared to the TMM prediction, and the results can be seen in Figure 6. The results are shown in third-octave bands.

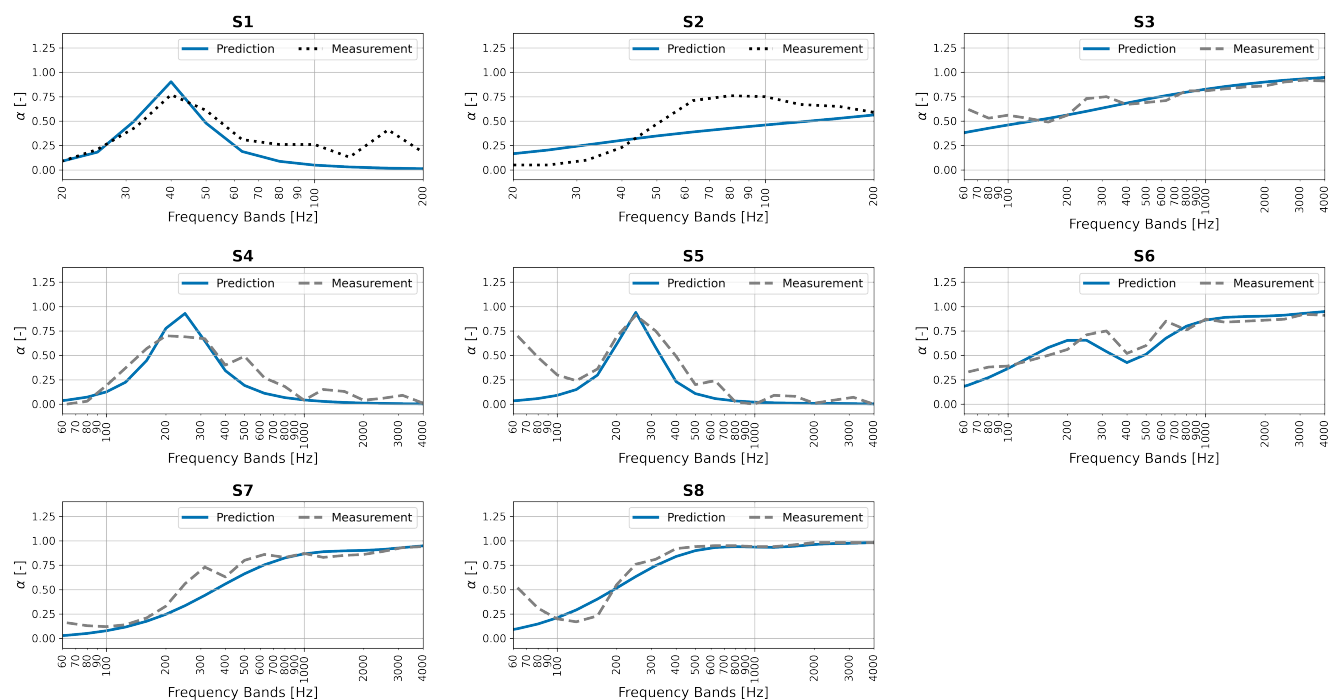


Figure 6 – Comparison between measurements and analytical prediction for the test samples. The solid blue curves are the TMM predictions, the dotted black curves are measurements in the 60 cm² tube and the gray dashed curves are measurements in the 16 cm² tube.

Except for sample S2, all the measured samples showed good agreement with the predictions. We believe that the errors seen on this sample might be due to the fact that four 50 mm samples of fiberglass were used to obtain the thickness of 200 mm, since a 200 mm sample is not made available by the manufacturer. This could have created an impedance discontinuity between the layers that allows each individual sheet to vibrate independently. The measurement results of samples S3, S5, S7 and S8 showed an over-estimated absorption coefficient at low-frequencies in comparison to the predictions, which the authors believe to be due to the boundaries of the tube not being massive and stiff enough to provide sufficient isolation at 63 Hz, causing a low-frequency energy leakage.

5 Conclusion

Even though the transfer matrix model method takes into account several simplifications and does not include important construction aspects of the absorbers, the absorption coefficient measurements showed good agreement with the predicted values.

The differences between the predictions and the measurements in lower frequencies are believed to be due to the fact that the equivalent fluid model used is only valid to frequencies higher than 45 Hz. Most of the analytical models involving porous material were not studied or developed to work at frequencies below 100 Hz. This ends up being a great source of uncertainty on the simulation of low-frequency absorbers, and more reliable results could be obtained with an equivalent fluid model designed to work in this frequency region. At higher frequencies, on the other hand, the differences are believed to be due to material properties, like tortuosity and porosity, that the empirical model does not take into account.

It is important to notice that, even though small differences are observed, the agreement between model and prediction is satisfactory even outside the frequency range of the chosen equivalent fluid model. Moreover, the method is considerably faster than numerical methods like FEM and BEM, which will take into account some of the aspects that are overlooked in the TMM approach, but are computationally costly.

The authors believe the Transfer Matrix Model representation, due to its speed and the good results when comparing to measured data, is a suitable method to be used as part of the Non-cuboid Iterative Room Optimizer software and other simulation methods that require complex surface impedances or absorption coefficients as input.

6 Future Work

Due to limited time and resources, only a small set of samples were measured. Based on the small number of samples tested, it is not possible to conclude whether the differences between the theoretical predictions and the measurements are coming from limitations on the analytical model or on the measurement set-up. A larger set of absorbers will be measured and repeatability tests with both impedance tubes will be made in order to have a larger and more reliable data set.

Acknowledgements

The authors would like to thank RPG Acoustic Systems and Walters-Storyk Design Group for their assistance in this research.

References

- [1] Allard, J. F.; Atalla, N. *Propagation of Sound in Porous Media: Modelling Sound Absorbing Materials*. 2nd ed. Wiley, 2009. ISBN: 97804707466150.

- [2] Cox, T.; D'Antonio, P. *Acoustic Absorbers and Diffusers: Theory, Design and Application*. 3rd ed. CRC Press, 2016. ISBN: 9781315352220. URL: <https://books.google.com.br/books?id=gi-LDQAAQBAJ>.
- [3] D'Antonio, P.; Jeong, C. H.; Nolan, M. Design of a new test chamber to measure the absorption, diffusion, and scattering coefficients. In: *The Journal of the Acoustical Society of America* 144.3 (2018), pp. 1814–1814. DOI: 10.1121/1.5068001. eprint: <https://doi.org/10.1121/1.5068001>. URL: <https://doi.org/10.1121/1.5068001>.
- [4] Munjal, M. L. *Acoustics of Ducts and Mufflers*. 2nd ed. Wiley, 2014. ISBN: ISBN: 9781118443125.
- [5] Oliva, D.; Hongisto, V. Sound absorption of porous materials – Accuracy of prediction methods. In: *Applied Acoustics* 74.12 (2013), pp. 1473–1479. ISSN: 0003-682X. DOI: <https://doi.org/10.1016/j.apacoust.2013.06.004>. URL: <https://www.sciencedirect.com/science/article/pii/S0003682X13001382>.
- [6] Petrolli, R. TMM - Toolbox for design and prediction of multilayered acoustic treatments. (accessed July 2021). URL: <https://github.com/rinaldipp/tmm>.
- [7] Petrolli, R. et al. Non-cuboid Iterative Room Optimizer. In: *Forum Acusticum*. HAL, Dec. 2020, pp. 1595–1602. DOI: 10.48465/fa.2020.0033. URL: <http://usir.salford.ac.uk/id/eprint/59744/>.
- [8] Scavone, G. An Acoustic Analysis Of Single-Reed Woodwind Instruments With An Emphasis On Design And Performance Issues And Digital Waveguide Modeling Techniques. In: 1997.